Science **217**, 364 (1982); T. L. Hopkins, T. D. Morgan, K. J. Kramer, *Insect Biochem.* **14**, 533 (1984); T. D. Morgan *et al.*, *ibid.*, in press; C. R. Roseland, J. M. Green, L. M. Riddiford, *J. Insect Physiol.* **32**, 473 (1986).
25. M. D. Sefcik, E. O. Stejskal, R. A. McKay, J. Schaefer, *Macromolecules* **12**, 423 (1979).
26. T. Kato, S. Ito, K. Fujita, *Biochim. Biophys. Acta* **881**, 415 (1986).
27. This is an isotropic chemical shift. A minor peak near 190 ppm also appears in the spectrum of the *ring*-^{13}C labeled cuticle (Fig. 4F), but this peak is a spinning sideband not removed by pulse techniques because of extensive ^{13}C–^{13}C dipolar coupling among aromatic carbons.
28. Research conducted by U.S. Grain Marketing Research Laboratory, Agricultural Research Service, U.S. Department of Agriculture, in cooperation with Monsanto Company and the Departments of Biochemistry and Entomology, Kansas Agricultural Experiment Station, Manhattan 66506 (contribution 87-51-J). Supported in part by grants 85-CRCR-1-1667 from the USDA Competitive Research Grant Program and PCM-8411408 from the National Science Foundation. Mention of a proprietary product in this paper does not imply approval by the USDA to the exclusion of other products that may also be suitable.

2 September 1986; accepted 15 December 1986

Isolation and Structure of a Covalent Cross-Link Adduct Between Mitomycin C and DNA

MARIA TOMASZ,* ROSELYN LIPMAN, DONDAPATI CHOWDARY, JAN PAWLAK, GREGORY L. VERDINE,† KOJI NAKANISHI*

A DNA cross-link adduct of the antitumor agent mitomycin C (MC) to DNA has been isolated and characterized; the results provide direct proof for bifunctional alkylation of DNA by MC. Exposure of MC to *Micrococcus luteus* DNA under reductive conditions and subsequent nuclease digestion yielded adducts formed between MC and deoxyguanosine residues. In addition to the two known monoadducts, a bisadduct was obtained. Reductive MC activation with $Na_2S_2O_4$ (sodium dithionite) leads to exclusive bifunctional alkylation. The structure of the bisadduct was determined by spectroscopic methods that included proton magnetic resonance, differential Fourier transform infrared spectroscopy, and circular dichroism. Formation of the same bisadduct in vivo was demonstrated upon injection of rats with MC. Computer-generated models of the bisadduct that was incorporated into the center of the duplex B-DNA decamer d(CGTACGTACG)$_2$ indicated that the bisadduct fit snugly into the minor groove with minimal distortion of DNA structure. A mechanistic analysis of the factors that govern monofunctional and bifunctional adduct formation is presented.

THE POTENT ANTITUMOR AGENT MITOMYCIN C (MC, **1**) is one of the few antibiotics known to react covalently with DNA in vivo and in vitro (*1*). Thus exposure of DNA to MC results in irreversible association of the MC chromophore with that of the DNA (*2*) and in altered

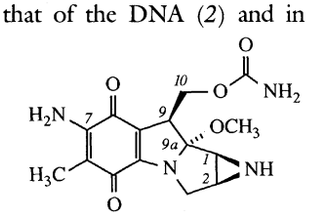

MC, **1**

renaturation kinetics due to putative formation of interstrand cross-links (*3*). However, since the proposed bifunctional cross-link or cross-links account for only a small fraction of the MC bound to DNA (*4, 5*), monofunctional binding is the major pathway under conditions that have normally been used.

The DNA-alkylating function of MC can be activated by two mechanisms: (i) reductive activation by bacterial and mammalian reductases or chemical reducing agents (*6–8*), and (ii) acidic activation by mild aqueous acid (*9, 10*). The structure of the major monofunctional adduct isolated from an MC-DNA complex has only recently been characterized as N^2-(2″β,7″-diaminomitosen-1″α-yl)-2′-deoxyguanosine (**2a**) (*11, 12*), a compound previously isolated from a model reaction and fully elucidated by spectroscopy (*13–16*). Adduct **2a** accounted for more than 90% of the MC bound to calf thymus DNA when the reductive activating agents NADPH–cytochrome c reductase/NADPH, xanthine oxidase/NADH, or H_2/PtO_2 were used in vitro; two minor N^2-dG adducts, **2b** and **3**, were also characterized. However, in that none of the above compounds corresponded to a mitosene ad-

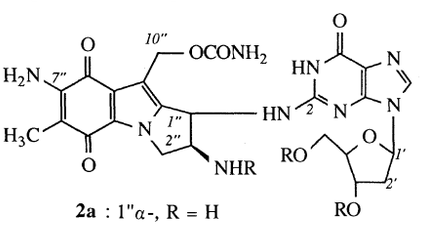

2a : 1″α-, R = H

2b : 1″ß-, R = H

2c : 1″α-, R = Ac

2d : 1″ß-, R = Ac

3 : 1″α-, R = H, 10″ substituent = -OH

duct (M)(*12*) bearing two attached nucleoside units ("cross-link"), the bifunctional adduct or adducts may have been formed in amounts too low for HPLC-UV detection. We found that the reducing system influences how MC reacts, whether as a monofunctional or bifunctional DNA-alkylating agent. We secured sufficient amounts of a bisadduct from reactions of MC with *Micrococcus luteus* DNA to fully characterize this bifunctional MC-DNA adduct.

Figure 1 shows HPLC traces of digestion mixtures that arose from MC–*M. luteus* DNA and MC-poly(dG-dC) complexes (*17*) that were formed under reductive activation by H_2/PtO_2 or $Na_2S_2O_4$. Activation of MC by H_2/PtO_2 (Fig. 1A) resulted in the production of four adducts from *M. luteus*

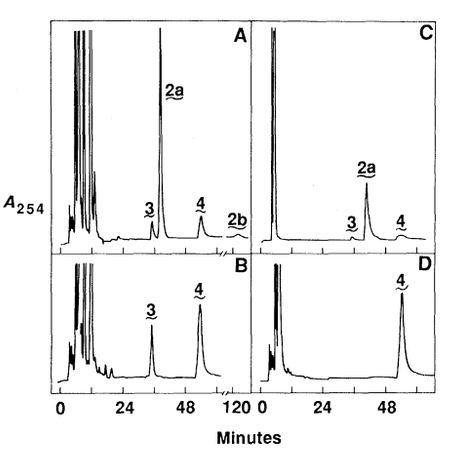

Fig. 1. HPLC patterns from DNase I, SVD, and alkaline phosphatase digest of various MC-DNA and MC-poly(dG-dC) complexes. (**A** and **B**) Digests of MC–*M. luteus* DNA complexes formed under reductive activation by H_2/PtO_2 and $Na_2S_2O_4$, respectively. (**C** and **D**) Digests of MC-poly(dG-dC) formed under reductive activation by H_2/PtO_2 and $Na_2S_2O_4$, respectively. Column: Beckmann Ultrasphere ODS, 1.0 by 25 cm; flow rate: 2.0 ml/min; eluant: 8/92 (v/v) CH_3CN/0.02*M* potassium phosphate, *p*H 5.0; detection: UV band at 254 nm (A_{254}).

M. Tomasz, R. Lipman, D. Chowdary, Department of Chemistry, Hunter College, City University of New York, New York, NY 10021.
J. Pawlak, G. L. Verdine, K. Nakanishi, Department of Chemistry, Columbia University, New York, NY 10027.

*Correspondence may be addressed to either of these authors.

†Present address: Department of Chemistry, Massachusetts Institute of Technology, Cambridge, MA 02139.

DNA; the major component was the 1''α-N^2-adduct **2a** and the minor components were (i) the 10''-decarbamoyl adduct **3**, (ii) the 1''β-N^2-adduct **2b**, and (iii) a bifunctional adduct **4**. The same set of adducts were formed with poly(dG-dC) under identical MC activation conditions (Fig. 1C), although the binding ratios were different in the two complexes (*11*) because of their different G and C contents.

The adduct patterns were strikingly different, however, when $Na_2S_2O_4$ (sodium dithionite) was used to reductively activate MC (*17*). Dithionite reduction of a mixture of MC and *M. luteus* DNA yielded no detectable amount of **2a**; instead, the predominant adducts were **3** and **4**, along with a new minor peak at 22 minutes in the case of DNA (Fig. 1B). The 22-minute peak was not identified but appeared closely related to **3** (*18*). More surprisingly, when poly(dG-dC) was treated with MC activated with $Na_2S_2O_4$, the bifunctional adduct **4** was the sole product of alkylation (Fig. 1D). Large-scale preparation of **4** is described in (*19*). The structure of **4** was determined as follows.

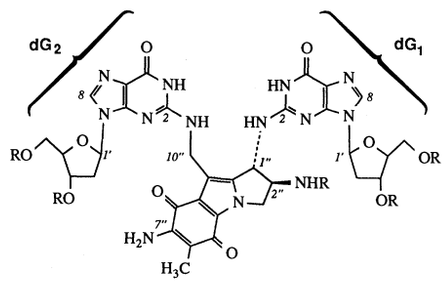

As shown in Fig. 2A, the UV spectra of bisadduct **4** consists of a summation of the mitosene (M) bands at 248, 315, 375, and 570 nm, and deoxyguanosine (G) bands at 252 and 274 nm (shoulder); the ratio of the intensity of the 252 nm (G+M) to the 315 nm (M) bands is about 2.8. This ratio is about 2.3 in the UV spectra of monoadducts **2a** or **2b** and indicated that **4** contained two dG units per M.

The weak negative 572-nm Cotton effect in the CD of monoadduct **4** (Fig. 2B), which is caused by perturbation of the M 570-nm UV band by the C-1'' chiral center, defines the α-configuration at C-1'' (*13*, *20*). This CD spectrum shows a distinct bisignate CD centered around 252 nm (Fig. 2B, stippled area), and is near the 252-nm UV maximum of the dG chromophore. Although this negative exciton-split CD (*21*) cannot define the absolute chirality of the two dG chromophores (because their electric transition moments are unknown), it

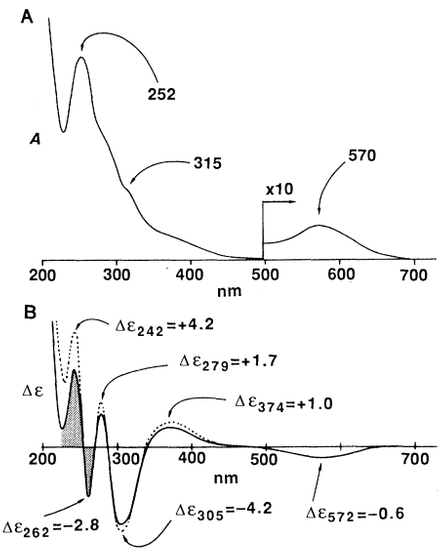

Fig. 2. (**A**) Ultraviolet spectrum of bisadduct **4** in 0.0*1M* potassium phosphate buffer, *p*H 7.0. (**B**) Comparison of CD spectra of bisadduct **4** derived from digestion of MC–*M. luteus* complexes that were formed under differing activation conditions. Solid line: H_2/PtO_2 activation; dashed line: $Na_2S_2O_4$ activation. The shaded peak denotes exciton-split CD that was caused by through-space interaction of the two dG chromophores. The Cotton effect at 572 nm defines the C-1''α-stereochemistry of **4**. Solvent; 0.0*1M* potassium phosphate, *p*H 7.0.

indicates that **4** contains two spatially proximal dG chromophores. This conclusion is supported by the lack of an exciton-split CD in the spectrum of monoadducts **2a** and **2b** (*20*).

Adduct **4** was peracetylated under standard conditions (*14*) except that the reaction vessel was placed in an ultrasonic bath during reaction to dissociate aggregates. The structure of **4** was supported by the NMR spectra of its pentaacetate **4a** (*21*), which included twinning of pertinent peaks (8-H at 7.89 and 7.81 ppm and 1'-H at 6.09 and 6.02 ppm). Proof of the linkage points was obtained by decoupling experiments. Thus decoupling of the exchangeable proton at 7.13 ppm (N^2-H in G_1) led to collapse of the M 1''-H at 5.13 ppm, while irradiation of another exchangeable proton at 6.50 ppm (N^2-H in G_2) led to the unveiling of an AB-quartet centered at 4.65 and 4.41 ppm (the two 10''-Hs). The lack of a 10''-carbamate NH_2 peak (usually ~6.5 ppm) combined with the 0.5-ppm upfield shift of the two 10''-H_2 signals indicated nucleophilic substitution by dG_2 at C-10''. Many common features were apparent in the ^{1}H-NMR spectra of mono- and bisadduct peracetates **2c** (*14*) and **4a** (*22*).

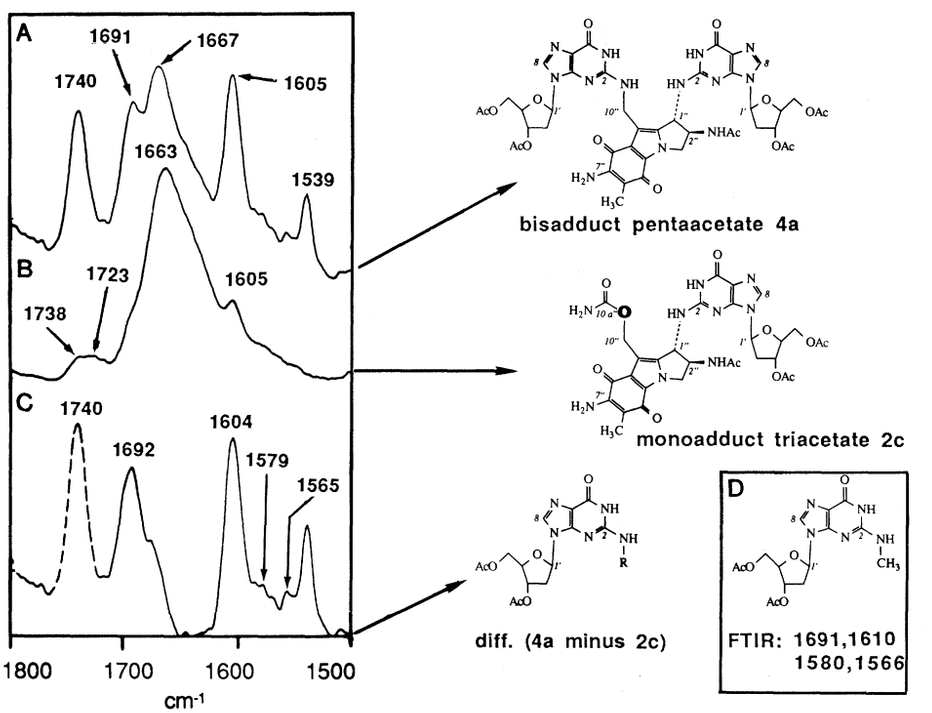

Fig. 3. The 1800 to 1500 cm^{-1} region solution FTIR spectra of (**A**) **4a**; (**B**) **2c**; and (**C**) weighted difference of **4a** minus **2c**. The difference spectrum in (C) shows peaks that are characteristic of N^2-substituted guanosines, as exemplified by N^2-methylguanosine triacetate (**D**), and indicates that the dG_2 moiety is MC-alkylated at its N^2-position. The dashed peak at 1740 cm^{-1} in (C) arises from the acetate carbonyl absorptions of dG_2. Because of the relative weakness of carbamate carbonyl absorptions, a discrete negative peak that arises from subtraction of the carbamate group in **2c** is not observed at 1722 cm^1. The spectrum was obtained in perdeuterated DMSO solution as described (*14*).

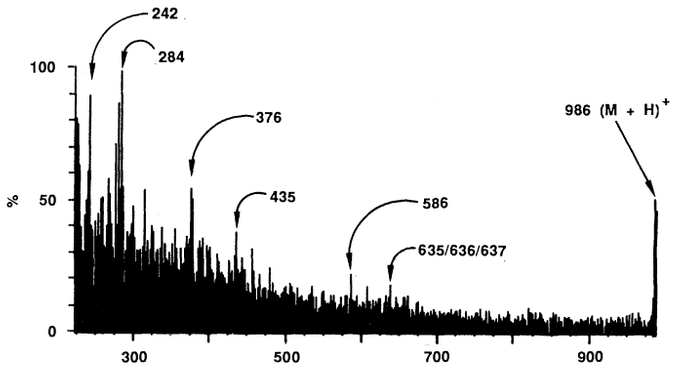

Fig. 4. Fast-atom-bombardment MS of bisadduct pentaacetate **4a**. Instrument, VG 70EQ; ionization gas, xenon; matrix, glycerol; sample size, ~0.1 μg. Some peaks showed clustering, an indication of quinone reduction during the ionization process.

The combination of solution FTIR, in which a cylindrical internal reflectance cell was used, and weighted spectral subtraction led to a direct determination of the linkage position on the guanosines that bore complex alkyl groups (*14*). Subtraction of the solution FTIR of monofunctional adduct triacetate **2c** from that of bifunctional adduct pentaacetate **4a** directly provided the heterosubstitution site on the dG_2 subunit of derivative **4a**. Weighted spectral subtraction of **4a** (Fig. 3A) minus **2c** (Fig. 3B) was performed by nulling all of their common M bands in the region 1675 to 1625 cm^{-1}. The weak dG bands were overwhelmed by the intense M bands and made such a subtraction feasible. The difference spectrum (Fig. 3C) shows bands at 1692, 1604, 1579, and 1565 cm^{-1} that match the set of bands at 1691, 1610, 1580, and 1566 cm^{-1} that are characteristic of a N^2-substituted guanosine (Fig. 3D).

The fast-atom-bombardment mass spectroscopy (MS) of bisadduct pentaacetate **4a** is shown in Fig. 4. The molecular ion was seen at a mass-to-charge ratio (*m/e*) of 986 $[M + H]^+$ (the calculated molecular weight for $C_{43}H_{47}O_{15}N_{13}$ was 985). The *m/e* peaks at 635, 636, and 637 were from the loss of dG diacetate, while the species *m/e* 586 were formed by loss of both deoxyribose diacetate moieties. The *m/e* 435 peak corresponded to the loss of the elements of dehydrodeoxyribose diacetate ($C_9H_{12}O_5$). The ion at *m/e* 376 was from the loss of acetamide from the ion at *m/e* 435, which also eliminated guanine to produce the ion at *m/e* 284. The ion at *m/e* 242 resulted from loss of ketene from *m/e* 284. The fragmentation pathway presented above was established by MS-MS studies of monoadduct peracetate **2d**.

The same bisadduct **4** could be isolated from DNA from the liver of rats that had been injected with MC. Its identity with authentic **4** was established by (i) identical elution volume on Sephadex G-25, (ii) identical elution time on HPLC (54 minutes), and (iii) identical UV spectrum in HPLC buffer (similar to that in Fig. 2) (*23*).

The covalent structure of the bifunctional adduct **4** represents an unusual type of DNA cross-link in which the exocyclic 2-amino groups of two dG residues are bridged by an exogenous alkylating agent. The facile formation of **4** in poly(dG-dC) indicated that MC forms interstrand cross-links at two diagonally opposed dG residues in opposite strands in a CpG or GpC sequence. In natural DNA, a priori a third bifunctional alkylation sequence could occur—that is, GpG, in which intrastrand cross-links could form (scheme 1). Isolation of bisadduct **4** from digests of MC-modified poly(dG)·poly(dC) indicates that such intrastrand cross-links are formed in this polymer and therefore most likely in natural DNA as well (*24*).

We examined the stereochemical fit of the MC cross-link in duplex DNA by inspection of computer-constructed and energy-minimized molecular models. The cross-link was incorporated into the central CpG sequence of the computer-generated duplex decamer $d(GCATCGATGC)_2$; the simulated molecular structure for this CpG–cross-linked decamer (**4**-decamer) is shown in Fig. 5A (*25*). Immediately evident in this view is the fit of the mitosene moiety in the minor groove of B-DNA. The sugar-phosphate backbone in the vicinity of the cross-link was not greatly distorted. All glycosidic bonds had the usual *anti* configuration; all other backbone features at this locus were similar to those observed in unmodified B-DNA molecules (*26*). The integrity of G-C base-pairing was

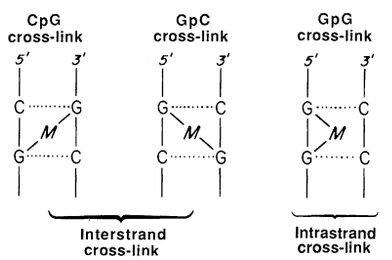

Scheme 1. Schematic representation of the three potential MC-DNA cross-linking sequences. M denotes the mitosene moiety.

maintained in both of the modified pairs, although the angles of propeller-twisting in the alkylated base pairs was somewhat altered. Additional features of the model are (i) the C_2N^2 bonds of the two cross-linked guanines (when viewed down the helix axis) appeared to be oriented in parallel in a manner similar to that in unmodified DNA (*25, 26*); and (ii) the mitosene 2″-ammonium function appeared to hydrogen-bond to three of the atoms on the same strand to which C-1″ is linked, that is, N3 and 3′-O of the 5′-dA and 4′-O of the 5′-dT (not clearly seen in Fig. 5A). It was also found that beneath the adduct the strand to which the mitosene C-1″ was linked underwent some reorganization to accommodate the 2″-ammonium group of the adduct. Measurements of the phosphorus-to-phosphorus distances across the minor groove revealed compression to widths of 8.1 and 9.5 Å in the region below the cross-link that gradually relaxed to the B-DNA–like values of 11.1 to 11.9 Å in the rest of the molecule (*25, 26*).

The snug fit of the mitosene unit in the CpG cross-link was demonstrated by examination of the van der Waals contacts that arose. The view of the van der Waals–surface model in Fig. 5B is directly along the minor groove. The α-face of the drug lies just within contact distance of the DNA backbone and thus rests firmly against it on one side. The drug appears to be relatively hidden in the groove, since its electronic shell protrudes less than 1 Å beyond the edges of the backbone. Furthermore, the mitosene 2″-ammonium group (Fig. 5B center, triplet of orange spheres) is located in a suitably spacious van der Waals pocket that is situated at the junction of the wall and floor on the β-face of the cross-link, and thus contributes significantly to the stability of the drug-DNA complex (*27, 28*).

The isolation and structural elucidation of the bifunctional MC-DNA alkylation product **4** constitutes the first direct chemical proof for formation of covalent cross-links between MC and DNA. The structure of **4** provides the first rigorous verification of the well-known Iyer-Szybalski hypothesis, which postulated the cross-linking functional groups of MC to be at its 1- and 10-positions (*6*). The observed influence of the mode of reduction of MC on its DNA-alkylating characteristics led to an understanding of the DNA cross-linking mechanism as follows.

Although $Na_2S_2O_4$, which selectively promoted bifunctional activation of MC, was a considerably stronger reducing agent than the others used in this study, all were capable of a full two-electron reduction of MC as well as mitosene derivatives (*29*). Therefore,

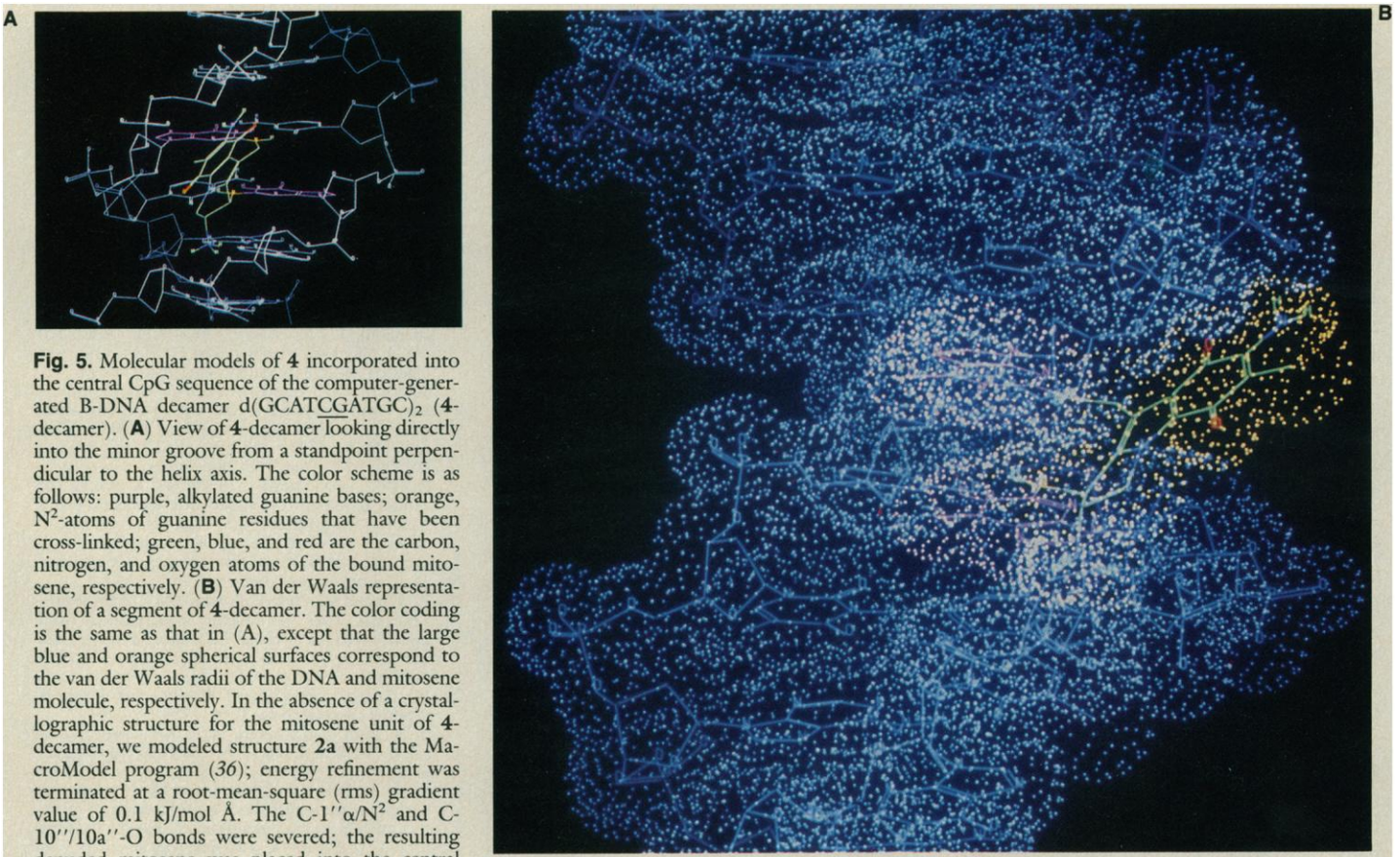

Fig. 5. Molecular models of **4** incorporated into the central CpG sequence of the computer-generated B-DNA decamer d(GCATCGATGC)$_2$ (**4**-decamer). (**A**) View of **4**-decamer looking directly into the minor groove from a standpoint perpendicular to the helix axis. The color scheme is as follows: purple, alkylated guanine bases; orange, N^2-atoms of guanine residues that have been cross-linked; green, blue, and red are the carbon, nitrogen, and oxygen atoms of the bound mitosene, respectively. (**B**) Van der Waals representation of a segment of **4**-decamer. The color coding is the same as that in (A), except that the large blue and orange spherical surfaces correspond to the van der Waals radii of the DNA and mitosene molecule, respectively. In the absence of a crystallographic structure for the mitosene unit of **4**-decamer, we modeled structure **2a** with the MacroModel program (*36*); energy refinement was terminated at a root-mean-square (rms) gradient value of 0.1 kJ/mol Å. The C-1′′α/N^2 and C-10′′/10a′′-O bonds were severed; the resulting denuded mitosene was placed into the central minor groove region of the computer-generated B-DNA decamer d(GCATCGATGC)$_2$. Bonds that linked the mitosene C-1′′ α- and C-10′′-positions to the N^2-atoms of the central CpG sequence of the decamer were introduced to form a crude version of **4**-decamer. This was then refined to an rms gradient value of 0.4 kJ/mol Å with the MacroModel minimization routines BDNR, SCCG, and PRCG, respectively, to generate the fully refined version of **4**-decamer shown in Fig. 5. The van der Waals surfaces were constructed (with the MacroModel "surface" option) on **4**-decamer to display 85% of the van der Waals radius of each atom; the value of 85% was chosen as it corresponds to that which is used by standard Corey-Pauling-Koltun models.

the reason for this selectivity does not simply lie in the differences of reducing strength among the various activators but rather in the following. The process of autocatalytic MC activation, in which nonstoichiometric reduction of MC resulted in stoichiometric activation of the drug, has recently been described (*30*). It has thus been clearly demonstrated that (i) MC activation can be performed catalytically in electron equivalents and (ii) the activation process is propagated in autocatalytic reactions by electron transfer from reduced mitosenes to the MC quinone. It is now apparent that the (in vitro) enzymatic- and H_2/PtO_2-type activation of MC has usually been conducted under autocatalytic conditions, since not all of the starting MC is consumed (*7*, *31*). In the case of $Na_2S_2O_4$ activation, however, no MC was recovered (*7*) and hence stoichiometric reduction and activation occurred. As an excess of reducing agent was present in all MC activation reactions ($Na_2S_2O_4$, flavoenzymatic, and H_2/PtO_2), the predominant factor that controls monofunctional versus bifunctional activation appears to be reduction kinetics rather than reduction thermodynamics.

The differential binding of MC to DNA under $Na_2S_2O_4$ reduction, as opposed to H_2/PtO_2 or flavoenzymatic reduction, can be rationalized. Subsequent to DNA alkylation, the activated monoadduct species **5** (*32*) can react further by two pathways

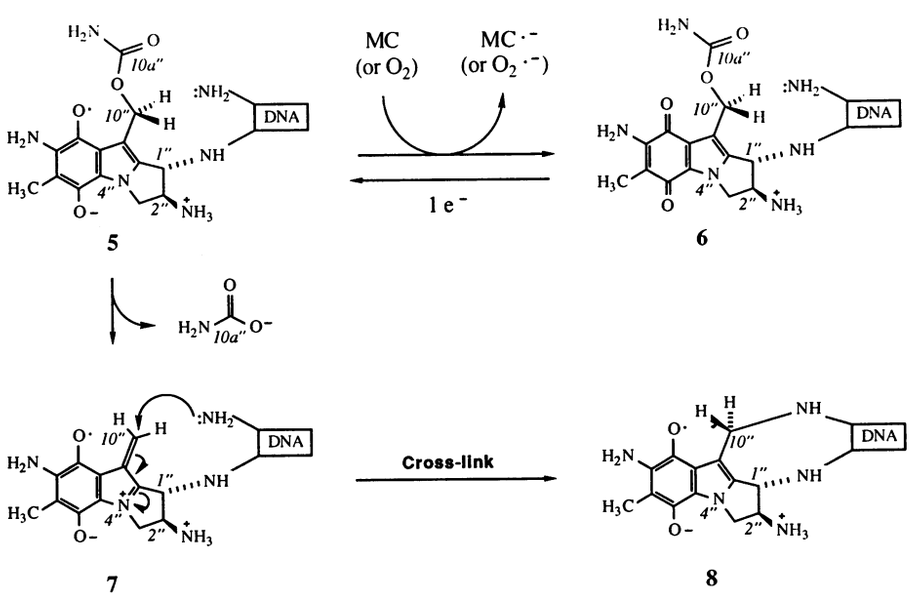

Scheme 2. Mechanism of DNA cross-linking by mitomycin C.

(scheme 2). In the first pathway, electron transfer from **5** to unreacted MC leads to quenching of the active species **5** and gives rise to the cross-link–incompetent quinone **6**; this reaction is thermodynamically favorable because of the difference in reduction potentials between mitosenes (such as **5**) and mitosanes [such as **1** (*29*)]. The conversion of **5** to **6** would be favored if excess MC were present, such as during the DNA alkylation reactions that use H_2/PtO_2 or flavoenzyme-catalyzed reactions (these reductions are slow). In the second pathway in the absence of excess MC, activated mitosene **5** is sufficiently long-lived to undergo a retro-Michael-type expulsion of carbamate to produce the iminium species **7** (*33*), which is attacked by a neighboring dG-N^2 atom to form the reduced cross-link **8** (or by H_2O to form reduced **3**). Because of the rapid kinetics of MC reduction by $Na_2S_2O_4$, the second pathway is presumably operative in alkylation reactions of MC that are promoted by $Na_2S_2O_4$. Even if **6** is formed in the initial stages, it will rapidly be reactivated to **5** because of the facile nature of $Na_2S_2O_4$ reduction. Thus, efficient bifunctional DNA alkylation in $Na_2S_2O_4$ activation occurs because the MC-reducing reaction in this case is much faster than in H_2/PtO_2 or flavoenzymatic activation. All of these mechanistic considerations given above should apply equally well to the hydroquinone forms of **5**, **7**, and **8**. There is mounting evidence, nonetheless, that suggests that one-electron reduction is sufficient to activate both electrophilic MC centers, namely C-1 (*34*) and C-10 (*31*).

The present findings also predict an effect of O_2, which is the specific inhibition of the bifunctional activation pathway due to inactivation of the active intermediate **5** by O_2 (scheme 2). This may be relevant to the greater toxicity of MC under hypoxic conditions, for example, to cells in solid tumors (*35*).

REFERENCES AND NOTES

1. Abbreviations: dG, deoxyguanosine; NAD(P)H, reduced nicotinamide adenine dinucleotide (phosphate); b.r., binding ratio in mole MC bound per mole mononucleotide unit; HPLC, high-performance liquid chromatography; UV, ultraviolet; CD, circular dichroism; NMR, nuclear magnetic resonance; DMSO, dimethyl sulfoxide; FTIR, Fourier transform infrared; N, nucleoside; 4-decamer, molecular model of DNA-bound bisadduct **4**; and E_0', standard redox potential. Abbreviations used in describing NMR data: ppm, parts per million; exch., exchangeable; br, broad; s, singlet; d, doublet; dd, doublet of doublets; and m, multiplet.
2. M. Tomasz, C. M. Mercado, J. Olson, N. Chatterjie, *Biochemistry* **13**, 4878 (1974).
3. V. N. Iyer and W. Szybalski, *Proc. Natl. Acad. Sci. U.S.A.* **50**, 355 (1963).
4. W. Szybalski and V. N. Iyer, *Microb. Genet. Bull. 16* (1964).
5. A. Weissbach and A. Lisio, *Biochemistry* **4**, 196 (1965).
6. W. Szybalski and V. N. Iyer, in *Antibiotics 1, Mechanism of Action*, D. Gottlieb and P. D. Shaw, Eds. (Springer, New York, 1967), pp. 211–245.
7. M. Tomasz and R. Lipman, *Biochemistry* **20**, 5056 (1981).
8. S. R. Keyes *et al.*, *Cancer Res.* **44**, 5638 (1984).
9. M. Tomasz, R. Lipman, G. L. Verdine, K. Nakanishi, *J. Am. Chem. Soc.* **107**, 6120 (1985).
10. M. Tomasz, R. Lipman, M. S. Lee, G. L. Verdine, K. Nakanishi, *Biochemistry*, in press.
11. M. Tomasz *et al.*, *Proc. Natl. Acad. Sci. U.S.A.* **83**, 6702 (1986).
12. The term "mitosene" refers to the structure as shown in **2** without substituents at C-1″, C-2″, and C-7″. In a less rigorous sense, we use it for 7″-aminomitosenes as well in this report.
13. We have reported that the mitosene moiety was linked to the O^6- rather than N^2-position of guanine. [M. Tomasz, R. Lipman, J. K. Snyder, K. Nakanishi, *J. Am. Chem. Soc.* **105**, 2059 (1983)]. Reinvestigation revealed that the correct structure is actually **2a** (*14*).
14. M. Tomasz, R. Lipman, G. L. Verdine, K. Nakanishi, *Biochemistry* **25**, 4337 (1986).
15. Shudo and co-workers have reported the isolation of two MC-dG adducts linked at N^2 and O^6 and an MC-dA adduct linked at N^6 [Y. Hashimoto, K. Shudo, T. Okamoto, *Acc. Chem. Res.* **11**, 403 (1984)]. However, some of the conclusions are in conflict with results of M. Tomasz *et al.* (*11*); the discrepancy is under investigation.
16. A recent study [S.-S. Pan, T. Tracki, N. R. Bachur, *Mol. Pharmacol.* **29**, 622 (1986)] described the major (monofunctional) MC-DNA adduct as having the mitosene linked to the O^6- rather than the N^2-position of dG. Since this conclusion was based on NMR comparisons with the adduct whose structure has recently been corrected to that of N^2-adduct **2a** (*14*), it follows that the major adduct isolated by Pan and co-workers from DNA treated with MC is presumably also **2a**.
17. Experimental details are as follows: (i) H_2/PtO_2 as activating agent: Treatment of *Micrococcus luteus* DNA (0.67 m*M* in nucleotides) with MC (0.335 m*M*) in neutral buffer at room temperature in the presence of H_2/PtO_2 (*11*) yielded an MC-DNA complex with a binding ratio (b.r.) of 0.05. The complex was digested by a mixture of deoxyribonuclease I, snake venom diesterase, and alkaline phosphatase; the digest was analyzed by HPLC (*11*). (ii) $Na_2S_2O_4$ as activating agent: *M. luteus* DNA (0.67 m*M* in nucleotides) and MC (0.335 m*M*) in neutral aqueous buffer were treated first with 0.06*M* aqueous $Na_2S_2O_4$ (1.5 mole per mole of MC) under anaerobic conditions (*2*) to yield an MC-DNA complex, b.r. 0.07, and then digested and analyzed by HPLC.
18. The UV spectrum of the 22-minute peak is identical to that of **3**. The 36-minute peak (**3**) had identical HPLC elution time, UV spectra, and Sephadex G-25 column elution volume with those of authentic **3** (*11*). The samples of adduct **4** obtained from all reactions (Fig. 1, A through D) were identical to each other and to authentic **4**, as concluded from identities of HPLC elution time, UV spectra, and the highly characteristic CD spectra (see Fig. 2B).
19. An MC-DNA complex (b.r. 0.20) was prepared from *M. luteus* DNA (160 mg) and MC (320 mg) under $Na_2S_2O_4$ activation; the resulting complex was digested. Separation was accomplished by preparative scale Sephadex G-25 (superfine) chromatography. Column: 5.0 by 56 cm; eluant: 0.02*M* ammonium bicarbonate, *p*H 8.5. Approximately 40 mg of complex was dissolved in 75 ml of buffer and loaded into the column per batch. The three fractions eluting after the deoxyribopurine nucleoside (dPu) fraction were identified by HPLC analysis as (i) the 22-minute adduct [not identified (*18*)], (ii) the 10′-decarbamoyl adduct **3**, and (iii) the bifunctional adduct **4**. These assignments were confirmed by comparison with authentic standards. The bifunctional adduct **4** was obtained after lyophilization as 4 mg of a homogeneous purple solid.
20. M. Tomasz, M. Jung, G. L. Verdine, K. Nakanishi, *J. Am. Chem. Soc.* **106**, 7367 (1984).
21. N. Harada and K. Nakanishi, *Circular Dichroism Spectroscopy—Exciton Coupling in Organic Stereochemistry* (University Science Books, Mill Valley, CA, 1983).
22. The ^{1}H-NMR of bisadduct pentaacetate **4a** (in perdeuterated DMSO) is as follows [chemical shift (multiplicity, integration), assignment]: 10.77, 10.54 ppm (exch. br s, 2H), N1-Hs; 8.52 (exch. d, 1H), 2″-NH; 7.89, 7.81 (br s, 2H), 8-Hs; 7.13 (exch. br d, 1H), 2-NH (G_1); 6.63 (exch. br s, 2H), 7″-NH_2; 6.49 (exch. br d, 1H), 2-NH (G_2); 6.09, 6.02 (dd/ddd, respectively, 2H), 1′-Hs; 5.28 to 5.16 (m, 2H), 3′-Hs; 5.16 (dd, 1H), 1″-H; 4.68 (dddd, 1H), 2″-H; 4.65 (dd, 1H), 10 ″-H_b; 4.51 (dd, 1H), 3″-H_b; 4.41 (dd, 1H) 10″-H_a; 4.25 to 4.05 (m, 6H), 4′-Hs and 5′-H_2s; 4.00 (dd, 1H), 3″-H_a; 2.95 to 2.70 (m, 2H), 2′-H_bs; 2.01, 1.99, 1.97 (s, 12H), methyl group of acetate; 1.79 (s, 3H), methyl group of 2″-acetamide; 1.75 (s, 3H), 6″-CH_3.
23. In a typical experiment, a fasted male Sprague-Dawley rat (185 g) was injected intraperitoneally with 15 mg of MC in 1.5 ml of 0.15*M* KCl twice, at a 2-hour interval, and killed 1 hour after the second injection. Liver nuclei and their DNA were isolated as described [R. G. Croy, J. M. Essigmann, V. N. Reinhold, G. N. Wogan, *Proc. Natl. Acad. Sci. U.S.A.* **75**, 1745 (1978)]. The DNA (11 mg) was digested and the digest was chromatographed over Sephadex G-25 exactly as in (*11*). No UV absorbance was detectable in the elution region corresponding to the elution volume of authentic standard (2250 to 3050 ml). Nevertheless, this fraction was collected, lyophilized, and applied in its entirety to HPLC (conditions as in Fig. 1). A peak at the elution time that corresponded to authentic **4** (54 minutes) was collected (0.55 A_{260} units) and its UV spectrum was determined. Control experiments with liver DNA of untreated rats gave negative results.
24. M. Tomasz, unpublished results.
25. R. Wing *et al.*, *Nature (London)* **287**, 755 (1980). The crystallographic structure was retrieved from the Brookhaven National Laboratory Protein Data Bank; F. C. Bernstein *et al.*, *J. Mol. Biol.* **112**, 535 (1977).
26. W. Saenger, *Principles of Nucleic Acid Structure* (Springer-Verlag, New York, 1984).
27. S. N. Rao, U. C. Singh, P. A. Kollmann, *J. Am. Chem. Soc.* **108**, 2058 (1986), and references therein.
28. P. A. Kollmann and co-workers have recently reported the molecular modeling of a series of hypothetical MC adducts incorporated into the decamer d[$(CG_5]_2$. Adduct **4** was modeled at a GpC sequence, and therefore the results of Kollman and co-workers are not directly comparable to ours, although a qualitative agreement is apparent (*27*).
29. Redox potentials (E_0') compared to the standard hydrogen electrode are as follows: $Na_2S_2O_4$, −660 mV [2e^-; S. G. Mayhew, *Eur. J. Biochem.* **85**, 535 (1987)];H_2/PtO_2, −414 mV; xanthine oxidase, −301 mV [lower E_0' of its two centers; R. Hill and V. Massey, *J. Biol. Chem.* **261**, 1241 (1986)]; NADPH–cytochrome c reductase, −371 mV [lowest E_0' of its four centers; T. Yanagi, N. Makino, H. S. Mason, *Biochemistry* **13**, 1701 (1974)]; MC, −126 mV (2e^-), and 2β,7-diamino-1-hydroxymitosene, −226 mV [2e^-; G. M. Rao, A. Begleiter, J. W. Lown, J. A. Plambeck, *J. Electrochem. Soc.* **124**, 199 (1977)].
30. D. M. Peterson and J. Fisher, *Biochemistry* **25**, 4077 (1986).
31. P. A. Andrews, S.-S. Pan, N. R. Bachur, *J. Am. Chem. Soc.* **108**, 4158 (1986).
32. The mechanism of reductive activation of MC that leads to an intermediate such as **5** has been described numerous times [see, for example, (*7*)].
33. N. Zein and H. Kohn, *J. Am. Chem. Soc.* **108**, 296 (1986).
34. S. J. Danishefsky and M. Egbertson, *ibid.*, p. 4648.
35. A. C. Sartorelli, *Biochem. Pharmacol.* **35**, 67 (1986).
36. MacroModel is a molecular mechanics program developed by C. Still (Chemistry Department, Columbia University) that executes simulation and energy minimization routines on small molecules as well as macromolecules. In addition, it can retrieve and manipulate structures that are deposited with the Brookhaven National Laboratory Protein Data Bank (*25*). The decamer d$(GCATCGATGC)_2$ was built with the MacroModel "grow" mode. All energy minimizations of **4**-decamer were performed with the AMBER program (*27*).

37. Supported by NIH grants CA 11572 (K.N.) and CA 28681 (M.T.) and a PSC-CUNY Faculty Research Award (M.T.). We thank G. Glick, W. Guida, and M. Lipton for assistance in performing calculations; G. Geller for assistance in gaining access to the Brookhaven Protein Data Bank; J. Barton, D. Patel, and G. Stork for helpful discussions; and C. Still for valuable discussions, helpful comments on the manuscript, and usage of computing facilities.

1 October 1986; accepted 20 January 1987